Superconductor Science and Technology

ACCEPTED MANUSCRIPT

Evaluation of a solid nitrogen impregnated MgB_2 racetrack coil

To cite this article before publication: Dipak Patel *et al* 2018 *Supercond. Sci. Technol.* in press https://doi.org/10.1088/1361-6668/aad9e0

Evaluation of a solid nitrogen impregnated MgB_2 racetrack coil

Dipak Patel[1,2], Wenbin Qiu[1], Mislav Mustapić[3], Jonathan C. Knott[1], Zongqing Ma[1], Daniel Gajda[4], Mohammed Shahabuddin[5], Jianyi Xu[6], Seyong Choi[7], Mike Tomsic[8], Shi Xue Dou[1], Yusuke Yamauchi[9], Jung Ho Kim[1] and Md Shahriar Al Hossain[1,9,10]

[1] Institute for Superconducting and Electronic Materials, Australian Institute for Innovative Materials, University of Wollongong, Squires Way, Innovation Campus, North Wollongong, New South Wales 2500, Australia

[2] School of Physics, University of New South Wales, Sydney, New South Wales 2052, Australia

[3] Department of Physics, University of Osijek, Trg Ljudevita Gaja 6, 31000 Osijek, Croatia

[4] Institute of Low Temperature and Structure Research, Polish Academy of Sciences, ul. Okólna 2, 50-422 Wrocław, Poland

[5] Department of Physics and Astronomy, College of Science, King Saud University, P.O. Box 2455, Riyad 11451, Saudi Arabia

[6] Ningbo Jansen NMR Technology Co., Ltd., No. 427 Gaoke Ave., Cixi New Industrial Area, Zonghan St., Cixi, Zhejiang, China

[7] Department of Electrical Engineering, Kangwon National University, Kangwon 25913, South Korea

[8] Hyper Tech Research, Inc., 539 Industrial Mile Road, Columbus, Oh 43228, USA

[9] Australian Institute for Bioengineering and Nanotechnology, University of Queensland, St Lucia 4072, Queensland, Australia

[10] School of Mechanical and Mining Engineering, University of Queensland, St Lucia 4072, Queensland, Australia

E-mail: md.hossain@uq.edu.au, jhk@uow.edu.au and y.yamauchi@uq.edu.au

Abstract

To develop powerful wind turbine generators using superconducting technology, high-performance superconducting racetrack coils are essential. Herein, we report an evaluation of a multifilamentary magnesium diboride (MgB_2) conductor-based racetrack coil cooled and impregnated simultaneously by solid nitrogen (SN_2). The coil was wound on a copper former with 13 mm winding width, an inner diameter of 124 mm at the curvature, and 130 mm length of the straight section. An *in situ* processed S-glass-insulated 36-filament MgB_2 wire was wound on the former in two layers with

19.5 turns, and heat treated via the wind and react method without any epoxy resin. The coil was evaluated for critical temperature and transport critical current in the SN_2 environment at different temperatures up to 31.3 K in self-field. The coil was able to carry 200 A transport current at 28.8 K in self-field. During coil charging and operation, SN_2 effectively acted as an impregnation material. The test results demonstrate the viability to use MgB_2 racetrack coil potentially with SN_2 impregnation in advanced rotating machine applications.

Keywords: MgB_2 conductor, racetrack coil, solid nitrogen impregnation, wind turbine generators

1. Introduction

Over usage of non-renewable energy sources around the globe has led to the serious problem of global warming. It is therefore imperative to maximize the use of renewable energy sources to keep global warming under control. Among the clean energy sources, wind power shows good potential for increasing cost-effective production capacity worldwide. In a windmill, a wind turbine uses a generator to harvest wind energy and convert wind energy into electric power.

At the end of 2015, the worldwide total capacity of wind energy production was approximately 432 GW [1]. In fact, more powerful turbines are required to raise wind power production and to minimize overall cost per unit generated energy from a windmill [2]. To meet this demand, off-shore wind turbine generators of up to 10-MW capacity with superconducting technology are being considered [3-13]. Superconducting windings can produce strong magnetic fields due to their ability to carry high current without any loss compared to copper (Cu) conductors. This means that using direct-drive machine design, more compact, lighter, more efficient, and more powerful wind turbine generators can be realized [2, 5, 11, 12, 14]. Several reviews have been published on the use of different types of superconductors for wind turbine application [6, 15]. Among the commercially available superconductors, magnesium diboride (MgB_2) with critical temperature (T_c) of 39 K has good potential to employ in rotating machines [6, 10, 12, 13, 16]. This is mainly due to its performance – cost ratio at around 20 K compared to high-temperature superconductors (HTS), and its availability in long piece-lengths [6, 14, 17].

In rotating machines, a racetrack coil configuration is used due to its electromagnetic and geometric advantages [4, 14, 18, 19]. To employ such superconducting coils in practical applications, however, extensive experimental validation is required to attain high coil performance. The first MgB_2-based racetrack coil was fabricated by Sumption *et al* using 42 m of monofilamentary wire via the wind and react method [20]. The coil achieved critical current (I_c) of 120 A in self-field at 4.2 K. Subsequently, using multifilamentary MgB_2 wire, Sumption *et al* fabricated another racetrack coil using the wind and react method [21]. At 5 K and 20 K, the coil reached I_c of 197 A and 95 A, respectively. Later, the same group also fabricated several racetrack coils using fully formed MgB_2 wires for the development of a 2-MW superconducting turbogenerator cooled by liquid-hydrogen [22]. One of the coils fabricated using monofilamentary MgB_2 wire attained I_c of 260 A in self-field at 20 K. The INWIND.EU project, funded under the FP7 framework, reported the design and winding aspects of an MgB_2 racetrack coil for a direct-drive 10-MW wind turbine generator pole [2, 8, 13]. Sarmiento *et al* reported the design and evaluation of a full-scale MgB_2 coil (one double pancake) for the 10-MW SUPRAPOWER wind turbine generators [10]. Their double pancake MgB_2 coil achieved I_c of 146.26 A, 133.59 A, and 91.79 A at 27.5 K, 28.5 K, and 30 K, respectively. We also fabricated two racetrack coils using monofilamentary MgB_2 conductor and tested them at 4.2 K [18]. These coils showed significant winding induced degradation. Coils for large-scale applications, however, will undoubtedly need a multifilamentary conductor to minimize ac losses. Thus, further work was essential on the fabrication process for multifilamentary MgB_2 racetrack coil to demonstrate high coil performance.

Moreover, the test results so far reported on MgB_2 racetrack coils have used either liquid helium (LHe) or a cryocooler (i.e. conduction cooling) for cooling purpose. In fact, a solid cryogen like solid nitrogen (SN_2) has also been considered for use as a cryogen for superconducting magnets [23-44]. SN_2 is known to improve the thermal stability of a superconducting magnet due to its high heat capacity [24, 27, 38, 41, 42]. In addition, due to its solid form, SN_2 can also act as an impregnation material in the superconducting magnet system to restrict the movement of the conductor while the coil is in operation [34]. This means that the mandatory requirement for epoxy impregnation in superconducting magnets can be eliminated [45]. SN_2 has been used as an impregnation material in solenoid and solenoid pancake coils [24, 34, 46]. SN_2 has not been used, however, as an impregnation material for racetrack coils. Solenoid coil winding is self-supported (i.e. due to winding tension) against expansion forces. In a racetrack coil, however, the winding at the straight section is not self-supported, and hence, external support is required to compensate for expansion forces during coil charging and operation [47]. Thus, it was necessary to evaluate SN_2 impregnation performance of a superconducting racetrack coil.

In this article, therefore, with a view towards the development of a pole coil for wind turbine generators and to explore the feasibility of using SN_2 for impregnation in MgB_2 racetrack coils, we present the fabrication and test results for an SN_2 impregnated racetrack coil fabricated via the wind and react method employing a multifilament MgB_2 conductor above 28 K in an SN_2 environment.

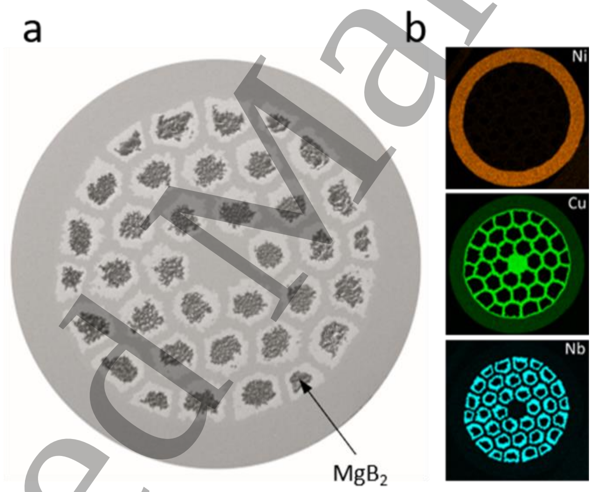

Figure 1. (a) Cross-sectional image of the multifilamentary MgB_2 wire (Platinum coating was deposited on the wire for imaging, thus contrast was not visible for Monel and Cu), (b) elemental maps for Ni, Cu, and Nb. Monel primarily consists of Ni and Cu.

2. Experimental details

The *in-situ* multifilamentary carbon (C)-doped MgB_2 conductor (strand no. 3520S) was supplied by Hyper Tech Research Inc. for the coil. The diameter of the wire was 1.1 mm, and 1.3 mm including the S-glass insulation. Each individual MgB_2 filament was surrounded by a niobium (Nb) barrier, and Cu was used as a stabilizer in the matrix.

Monel was used as an outer sheath. The conductor contained 36 filaments and one Cu filament at the centre. The filling factor of the conductor was 11.1 %. Figure 1(a) and (b) shows a cross-sectional image and elemental maps of the MgB_2 wire used for the coil winding.

To wind the coil, a Cu former with a racetrack profile was designed and fabricated. The former had a winding width of 13 mm, an inner diameter (I.D.) of 124 mm at the curvature, and a straight section with a length of 130 mm. To pass current through the coil conductor, two current terminals of 30 mm in diameter were fabricated. Ceramic washers were used to provide electrical insulation between the current terminals and the coil former. There was also an air gap between the current terminals and the coil former. The air gap between the terminals and the former was filled using insulated Cu and Stycast® 2850FT (Catalyst 9) after heat treatment of the coil to enhance the thermal contact.

Table 1. Specifications of the MgB_2 racetrack coil.

Parameters	**Specifications**
Coil type	Racetrack
Fabrication method	Wind and react
Strand (HTR 3520S)	MgB_2/Nb/Cu/Monel Nb: barrier, Cu: matrix, Monel: sheath
Strand type	*In situ*
Carbon content (wt. %)	2
Filament count	36 + 1 (Cu at centre)
Insulation	S-glass
Wire diameter with insulation (mm)	1.3
Wire diameter without insulation (mm)	1.1
SC fill factor of the wire (%)	11.1
Coil winding width (mm)	13
Coil I.D. at curvature (mm)	124.0
Coil O.D. at curvature (mm)	129.2
Length of the straight section (mm)	130.0
Turns per layer	19.5 (1^{st} : 10, 2^{nd} : 9.5)
Total layers	2
Heat treatment (°C·h^{-1})	675·1
Impregnation	No (only SN_2 while cooling down)

The coil was wound using 13 m wire in two layers with a total of 19.5 turns (1^{st} layer: 10 turns, 2^{nd} layer: 9.5 turns). One turn was wound on each current terminal to reduce electrical contact resistance between the current terminal and the MgB_2 wire [48]. The heat treatment of the coil was carried out at 675 °C for 1 h in an inert argon atmosphere, with a temperature ramp rate of 5 °C·min^{-1}. The coil was naturally cool down to room temperature following the heat treatment. After heat treatment, the utmost precautions were taken to avoid conductor movement. To measure the voltage drop during current charging, two pairs of voltage taps were installed across the coil. One pair of voltage taps were installed across the entire coil (V1, 12.74 m) and one pair across six turns in the outer layer (V2, 3.95 m). The coil was not impregnated using any epoxy. Table 1 shows the specifications of the MgB_2 racetrack coil, whereas figure 2(a) shows a digital image of the fabricated MgB_2 racetrack coil. The commercial wind turbine coils will have straight section much longer than the curvature diameter. Thus, it can be more difficult to keep the wire in the straight sections in place before the liquid nitrogen (LN_2) is frozen compared to this experimental coil.

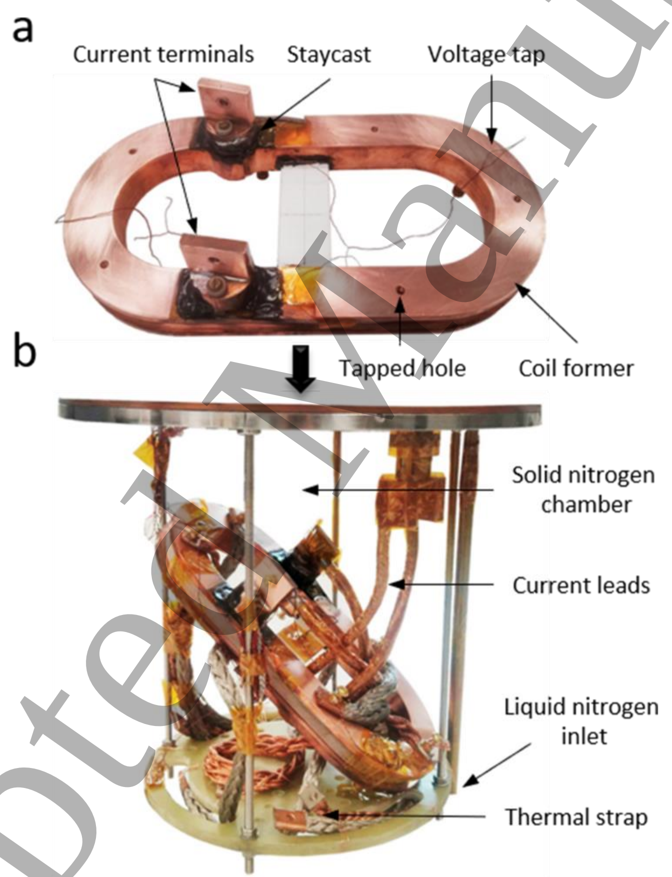

Figure 2. Digital images: (a) fabricated racetrack coil (wind and react), (b) racetrack coil in the SN_2 chamber.

To characterise the transport properties of the MgB_2 racetrack coil, the coil was mounted in the SN_2 chamber, as can be seen in figure 2(b). For further details of our SN_2 cooling system, see [43]. Due to space constraints, the coil was installed at an angle. In the SN_2 chamber, the LN_2 inlet is located at the bottom (see figure 2(b)).

Thus, there was a possibility that the coil could cool down unevenly because the bottom section of the coil would come into contact with the LN_2 first. A large gradient of temperature across the coil while cooling down from 300 K to 77 K could develop stress on the coil conductor, which could degrade its performance [21, 49]. Therefore, to keep the temperature gradient at a minimum while cooling down from 300 K to 77 K, ten Cu straps were installed on the coil former from the tapped holes (see figure 2(a)), as shown in figure 2(b). The flexible Cu leads were used to make the connection between the coil and current leads.

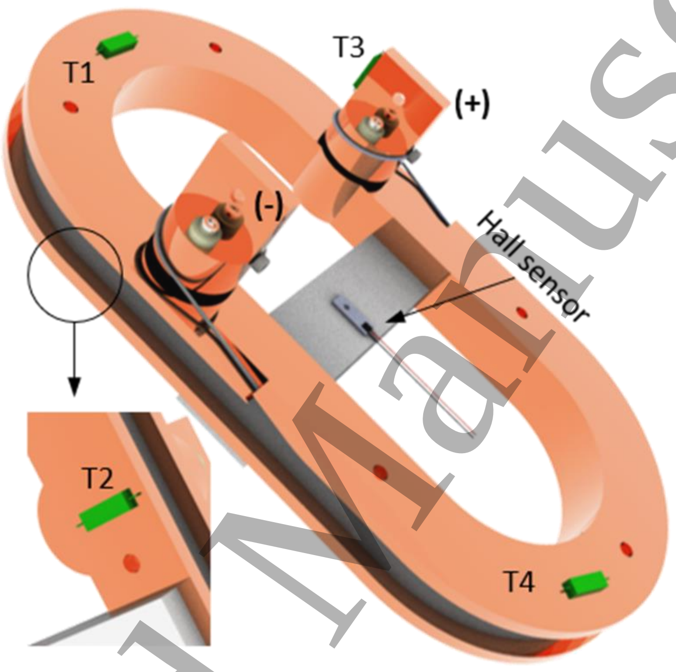

Figure 3. Schematic representation of the temperature and Hall sensor(s) on a 3D model of the racetrack coil. The Hall sensor was installed at the centre (at z = 0) of the coil. Temperature sensor locations are indicated (T1 – at the top of the former, T2 – at bottom of the former below current terminal, T3 – at the positive current terminal, and T4 – at the bottom of the former).

Figure 3 is a schematic representation of the temperature and Hall sensor(s) on a three-dimensional (3D) model of the racetrack coil. The magnetic field (*B*) at the centre of the coil at z = 0 was measured using a Hall sensor (0.1 G sensitivity). As shown in the figure, four carbon ceramic sensors (CCS) were also installed on the coil to monitor the temperature.

3. Results and discussion

Prior to cool down of the MgB_2 racetrack coil for transport measurements, finite element analysis (FEA) of the coil was performed to estimate the field constant, self-inductance, centre field (at z = 0), field distribution in the major and minor directions in the bore, and peak field on the coil in advance. A transport current of 200 A was used for the FEA simulations as that was the maximum limit of our power supply. The COMSOL Multiphysics software package was used for FEA simulations. The specifications of the fabricated coil were used to model the coil winding for the FEA simulations. At 200 A transport current, the field at the centre (at z = 0) of the coil and the total stored magnetic energy was estimated to be 0.0283 T and 3.29 J, respectively. These results indicate field constant and self-inductance of 1.415 $G \cdot A^{-1}$ and 165 μH, respectively. To further evaluate the field distribution in the bore of the coil at 200 A, the magnetic field density norm was plotted along the major (x) and minor (y) directions at z = 0, as shown in figure 4. In the x- and y-directions at z = 0, the peak fields were 0.191 T and 0.174 T, respectively. This means that the curvature region experienced 9.8 % higher field than the straight section at the given location. The inset of figure 4 shows the surface plot of the magnetic field density of the coil. As expected, the peak field on the surface of the coil was 0.2034 T (at 200 A) at the inner curvature. The FEA estimated parameters of the coil are shown in table 2.

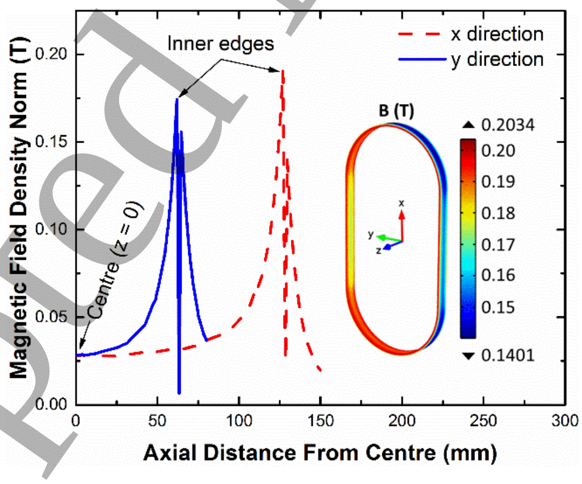

Figure 4. Magnetic field density norm versus axial distance from the centre profile in the coil at 200 A. The long and short sections of the coil are represented by x- and y directions, respectively. A surface plot of the magnetic field density is shown in the inset.

The SN_2 cooling system was evacuated (<2 × 10^{-6} Torr) using a turbomolecular pump to initiate the cool down of the coil [43]. Then, LN_2 was slowly introduced into the SN_2 chamber. The cryocooler was switched on when the temperature on its 2nd stage (attached to the SN_2 chamber) reached 280 K. The LN_2 transfer rate was manually controlled such that the temperature gradient across the coil during cool down remained as small as possible.

Table 2. FEA simulated and measured transport properties of the racetrack coil. The maximum (max.) and minimum (min.) are the temperatures on the coil while I_c measurement.

Parameters	Values
FEA simulated	
Field constant (G·A^{-1})	1.415
Inductance, *L* (μH)	165
Centre field at z = 0 (T) at 200 A	0.0283
Peak field (T) at 200 A	0.2034
Measured	
Field constant (G·A^{-1})	1.385
Inductance, *L* (μH)	179
Centre field at z = 0 (T) at 200 A	0.0277
T_c (K)	34.5
I_c (A) at max.: 28.8 K, min.: 27.6 K	>200
I_c (A) at max.: 30.3 K, min.: 29.7 K	147.0
I_c (A) at max.: 30.8 K, min.: 30.2 K	118.7
I_c (A) at max.: 31.3 K, min.: 30.7 K	90.1

Figure 5(a) and (b) shows the temperature versus time and the temperature gradient versus time profiles while cooling from 300 K to 77 K of the various temperature sensors installed on the racetrack coil, respectively. The time to cool down the coil from 300 K to 77 K was approximately 6 h, and the cool down was reasonably uniform (figure 5(a)). As can be seen in figure 5(b), the temperature gradients while cooling down from 300 K to 77 K were within ±5 K. Among the three temperature gradients, the temperature gradient between T1 and T2 was lowest, as they were installed geometrically close to each other. The positive current terminal was connected with current leads (see figure 2(b)) and a thermal strap was not installed on it. Thus, to cool down the current terminal, the entire flexible Cu lead needed to be cooled. This was the reason for the high temperature at the T3 location compared to T1. As a result, a negative temperature gradient was observed between

T1 and T3. As expected, the bottom section of the coil cooled first because it was in the vicinity of the LN_2 inlet (see figure 2(b)). Therefore, a positive temperature gradient was recorded between T1 and T4. Once the coil reached 77 K, the SN_2 chamber was completely filled with LN_2. The inlet of the chamber was closed, the non-returning valve was installed in the outlet, and further cool down was achieved using the cryocooler.

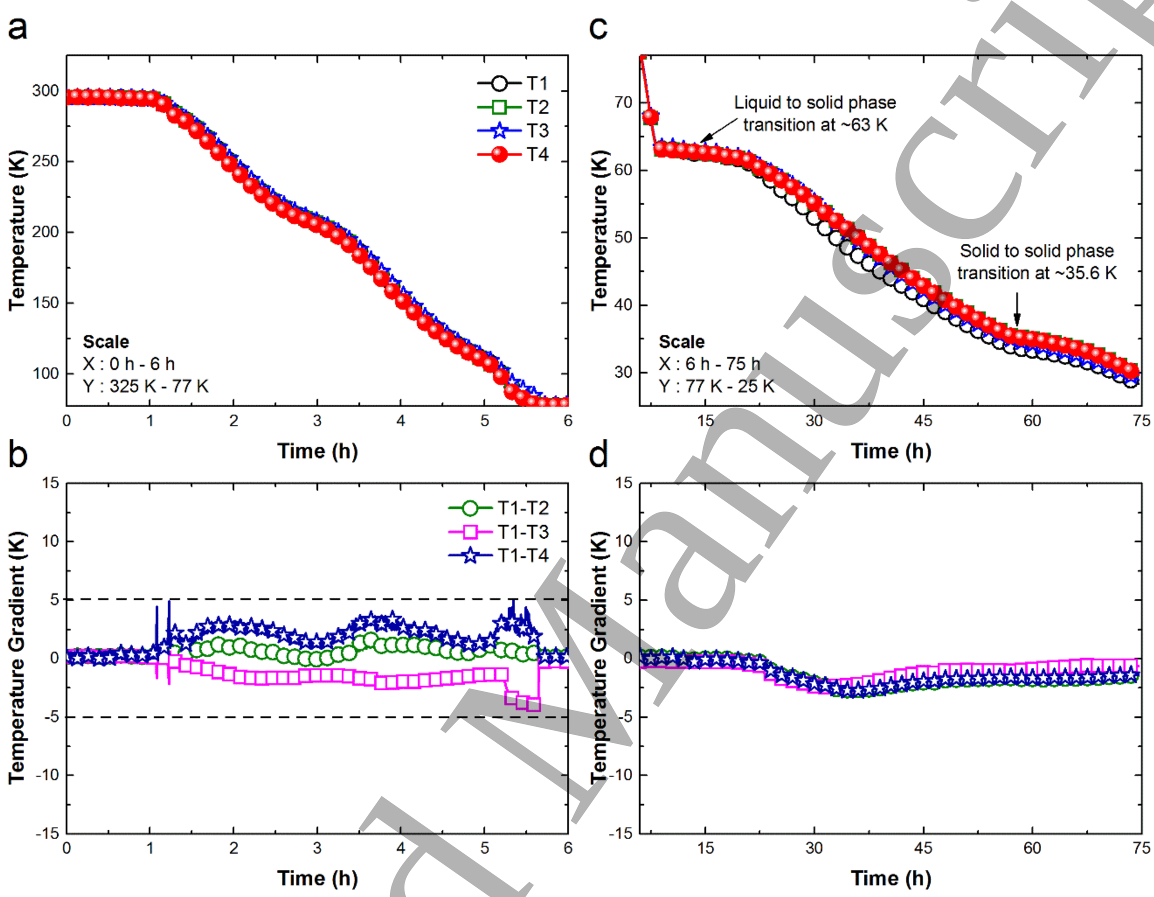

Figure 5. (a) Temperature versus time profiles from 300 K to 77 K, (b) temperature gradient versus time profiles from 300 K to 77 K, (c) temperature versus time profiles from 77 K to 28.3 K, and (d) temperature gradient versus time profiles from 77 K to 28.3 K during cool down of the coil in the SN_2 chamber. The cool down data are continuous in time. The legends in (a) and (c), and (b) and (d) are the same.

Like figure 5(a) and (b), figure 5(c) and (d) shows similar temperature profiles of the coil while cooling from 77 K to 28.3 K (the minimum temperature on the coil). As can be seen in figure 5(c), it took 69 h to cool down the coil from 77 K to 28.3 K. The two typical phase transitions of SN_2 were recorded at ~63 K (liquid to solid) and ~35.6 K (solid to solid) [45]. In the SN_2 chamber, after the liquid to solid phase transition at ~63 K, the temperature of the top section of the SN_2 was reduced first due to the proximity of the cooling source (i.e. the cryocooler) and the low thermal diffusivity of SN_2 [45]. The temperature gradients were negative, therefore, between T1 and T2; T1 and T3; and T1 and T4 while cooling down from 77 K (figure 5(d)).

While cooling down, T_c of the racetrack coil was evaluated by passing 100 mA constant current from 36.7 K. Figure 6(a) shows the resistance versus temperature profile of the coil. The temperature sensor at the bottom of the coil (T4) was taken as the reference temperature for this measurement because it was measuring the highest temperature on the coil during cool down. The measured T_c of the coil was 34.5 K. The T_c was consistent with the wire specification.

In the next step, the self-inductance and field constant of the coil was measured. For this purpose, a current of up to 10 A was passed through the coil at a ramp rate of 0.25 $A \cdot s^{-1}$, and the magnetic field at the centre of the coil and the voltage drop across the entire coil were recorded simultaneously. The measured field constant and self-inductance (based on the inductive voltage across the coil during coil charging) of the coil were 1.385 $G \cdot A^{-1}$, and 179 μH, respectively. These parameters were consistent with the FEA simulated parameters (see table 2).

To evaluate the transport properties of the racetrack coil, the I_c of the coil was measured by the standard four-probe method at 28.8 K (the highest temperature (T4) on the coil) using the 1 $\mu V \cdot cm^{-1}$ criterion, as shown in figure 6(b). At 28.8 K, in a self-field of 0.2034 T, the coil was able to carry 200 A current, which was the limit of the power supply. During the charging process, the temperatures on the coil remained constant. A slight temperature rise was observed on the current terminal, however, due to the mechanical connection between the current lead and the terminal. In comparison to our previously reported results on MgB_2 racetrack coils [18], the racetrack coil in this work showed significantly enhanced transport properties. To achieve high performance, several improvements were made in this work compared to our previous work. Firstly, in order to improve the strain tolerance and to avoid mismatch of the thermal expansion coefficient of the epoxy resin with that of the MgB_2 wire, in this work, we used multifilament wire without any epoxy impregnation [50]. Secondly, the coil fabrication process was optimized such that no conductor movement took place after heat treatment of the coil. The racetrack coil in this work was impregnated using only SN_2. This means that, as in a solenoid, in the racetrack coil, SN_2 also effectively acted as an impregnation material and held the conductors in place during operation. To the best of our knowledge, this work is the first to show a transport current as high as 200 A above 28 K in an MgB_2 racetrack coil test results reported so far.

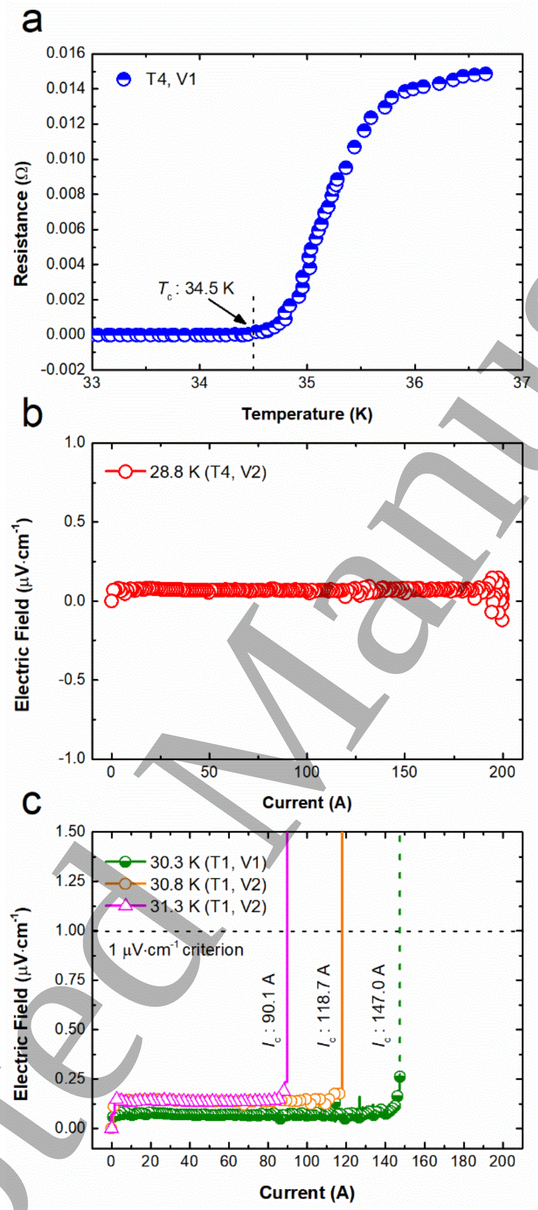

Figure 6. (a) Resistance versus temperature profile, electric field versus current characteristics (b) at 28.8 K (T4), and (c) at 30.3 K, 30.8 K, and 31.3 K (T1) for the racetrack coil. The dashed green line is the anticipated electric field line. The temperature sensor location T1 was at the top of the coil, and T4 was at the bottom of the coil. V1 and V2 represent the voltage taps across the entire coil and outer layer,

respectively. The current ramp rate at 30.3 K was 0.5 $A \cdot s^{-1}$, whereas, at 30.8 and 31.3 K, it was 1 $A \cdot s^{-1}$.

To further measure the transport properties of the coil above 28.8 K, the temperature of the coil was increased using a heater at the 2nd stage (attached to the SN_2 chamber) of the cryocooler. The temperature dependent I_c(s) of the coil is shown in figure 6(c). The I_c(s) values of the coil at 30.3 K, 30.8 K, and 31.3 K were 147.0 A, 118.7 A, and 90.1 A, respectively. The temperature sensor at the top of the coil (T1) was taken as a reference temperature for this measurement as it measured the highest temperature on the coil while the temperature was increasing. In the SN_2 chamber, as the temperature was rising, the temperature of the top section of the SN_2 was raised first due to the proximity of the heater, and the low thermal diffusivity of SN_2 [45]. As can be seen in figure 6(c), at 30.8 K and 31.3 K, very sharp quench like transitions from the superconducting to the normal state was observed in the outer layer. In contrast, the transition at 30.3 K across the entire coil was relatively smooth. As soon as the transition was observed, the current was decreased from 147 A to avoid irreversible damage in the coil due to the transient resistive heating at high currents. This indicates that the coil had an I_c of ~147 A at 30.3 K. The measured transport properties of the coil are listed in table 2. The expected I_c(s) of the coil at 15 K in 2 T and 25 K in 1 T would be around 221 A and 105 A, respectively based on the short-wire I_c measurement in LHe vapour cooling.

4. Conclusions

We fabricated and evaluated the transport properties of an SN_2 impregnated multifilamentary MgB_2-based racetrack coil above 28 K in self-field. Firstly, FEA simulations of the coil were carried out to estimate some of the critical parameters of the coil. The FEA simulated field constant, self-inductance, and centre field at z = 0 were 1.415 $G \cdot A^{-1}$, 165 μH, and 0.0283 T (at 200 A), respectively. These values were consistent with the measured values of 1.385 $G \cdot A^{-1}$, 179 μH, and 0.0277 T (at 200 A), respectively. In the next step, T_c of the coil was measured. The measured T_c of the coil was 34.5 K, which was consistent with the wire specification. Finally, the coil was evaluated for transport current up to 200 A at different temperatures. The transport current of the coil at 28.8 K, 30.3 K, 30.8 K, and 31.3 K was measured to be >200 A, 147 A, 118.7 A, and 90.1 A, respectively, at self-field. During current charging up to

200 A, SN_2 effectively acted as an impregnation material and held the conductors in place. According to the literature, this work is the first to show transport current as high as 200 A above 28 K in an MgB_2 racetrack coil. Such high performance of the coil demonstrates the suitability of MgB_2 racetrack coil potentially with SN_2 cooling for the application in future wind turbine generators.

Acknowledgements

This work was supported by the Australian Research Council (DE130101247, LP160101784), Australian Academy of Sciences' AISRF scheme, International Scientific Partnership at King Saud University through ISPP #0095, and International S&T Cooperation Program of China (ISTCP) 2015DFA13040. The authors would like to thank Dr. Tania Silver for helpful discussions.

References

[1] Global Wind Energy Council www.gwec.net (accessed June 2018).

[2] Magnusson N, Eliassen J C, Abrahamsen A B, Nysveen A, Bjerkli J, Runde M and King P 2015 Design aspects on winding of an MgB_2 superconducting generator coil *Ener. Proc.* **80** 56-62

[3] Abrahamsen A B, Mijatovic N, Seiler E, Zirngibl T, Træholt C, Nørgård P B, Pedersen N F, Andersen N H and Østergård J 2010 Superconducting wind turbine generators *Supercond. Sci. Technol.* **23** 034019

[4] Terao Y, Sekino M and Ohsaki H 2012 Electromagnetic design of 10 MW class fully superconducting wind turbine generators *IEEE Trans. Appl. Supercond.* **22** 5201904

[5] Abrahamsen A B, Magnusson N, Jensen B B and Runde M 2012 Large superconducting wind turbine generators *Ener. Proc.* **24** 60-7

[6] Jensen B B, Mijatovic N and Abrahamsen A B 2013 Development of superconducting wind turbine generators *J. Renew. Sustain. Energy* **5** 023137

[7] Liang Y C, Rotaru M D and Sykulski J K 2013 Electromagnetic simulations of a fully superconducting 10-MW-class wind turbine generator *IEEE Trans. Appl. Supercond.* **23** 5202805

[8] Abrahamsen A B, Magnusson N, Jensen B B, Liu D and Polinder H 2014 Design of an MgB_2 race track coil for a wind generator pole demonstration *J. Phys. Conf. Ser.* **507** 032001

[9] Sanz S, Arlaban T, Manzanas R, Tropeano M, Funke R, Kováč P, Yang Y, Neumann H and Mondesert B 2014 Superconducting light generator for large offshore wind turbines *J. Phys. Conf. Ser.* **507** 032040

[10] Sarmiento G, Sanz S, Pujana A, Merino J M, Marino I, Tropeano M, Nardelli D and Grasso G 2016 Design and testing of real-scale MgB_2 coils for SUPRAPOWER 10-MW wind generators *IEEE Trans. Appl. Supercond.* **26** 5203006

[11] American Superconductor www.amsc.com (accessed June 2018).

[12] Kalsi S S 2014 Superconducting wind turbine generator employing MgB_2 windings both on rotor and stator *IEEE Trans. Appl. Supercond.* **24** 5201907

[13] Magnusson N, Eliassen J C, Abrahamsen A B, Hellesø S M, Runde M, Nysveen A, Moslått L E, Bjerkli J and King P 2018 Fabrication of a scaled MgB_2 racetrack demonstrator pole for a 10-MW direct-drive wind turbine generator *IEEE Tran. Appl. Supercond.* **28** 5207105

[14] Marino I, Pujana A, Sarmiento G, Sanz S, Merino J M, Tropeano M, Sun J and Canosa T 2016 Lightweight MgB_2 superconducting 10 MW wind generator *Supercond. Sci. Technol.* **29** 024005

[15] Lloberas J, Sumper A, Sanmarti M and Granados X 2014 A review of high temperature superconductors for offshore wind power synchronous generators *Ren. Sus. Ener. Rev.* **38** 404-14

[16] Nagamatsu J, Nakagawa N, Muranaka T, Zenitani Y and Akimitsu J 2001 Superconductivity at 39 K in magnesium diboride *Nature* **410** 63-4

[17] Patel D, Hossain M S A, Motaman A, Barua S, Shahabuddin M and Kim J H 2014 Rational design of MgB_2 conductors toward practical applications *Cryogenics* **63** 160-5

[18] Kundu A, Patel D, Kumar N, Panchal A G, Qiu W, Jie H, Ma Z, Yanmaz E, Shahabuddin M, Kim J H, Pradhan S and Hossain M S A 2016 Fabrication, transport current testing, and finite element analysis of MgB_2 racetrack coils *J. Supercond. Nov. Magn.* 1-6

[19] Kajikawa K, Uchida Y, Nakamura T, Kobayashi H, Wakuda T and Tanaka K 2013 Development of stator windings for fully superconducting motor with MgB_2 wires *IEEE Trans. Appl. Supercond.* **23** 5201604

[20] Sumption M D, Bhatia M, Rindfleisch M, Phillips J, Tomsic M and Collings E W 2005 MgB_2/Cu racetrack coil winding, insulating, and testing *IEEE Trans. Appl. Supercond.* **15** 1457-60

[21] Sumption M D, Bohnenstiehl S, Buta F, Majoros M, Kawabata S, Tomsic M, Rindfleisch M, Phillips J, Yue J and Collings E W 2007 Wind and react and react and wind MgB_2 solenoid, racetrack and pancake coils *IEEE Trans. Appl. Supercond.* **17** 2286-90

[22] Sumption M D, Bhatia M, Buta F, Bohnenstiehl S, Tomsic M, Rindfleisch M, Yue J, Phillips J, Kawabata S and Collings E W 2007 Multifilamentary MgB_2-based solenoidal and racetrack coils *Physica C* **458** 12-20

[23] Haid B, Lee H, Iwasa Y, Oh S S, Ha H S, Kwon Y K and Ryu K S 2001 Stand-alone solid nitrogen cooled "permanent" high-temperature superconducting magnet system *IEEE Trans. Appl. Supercond.* **11** 2244-7

[24] Isogami H, Haid B J and Iwasa Y 2001 Thermal behavior of a solid nitrogen impregnated high-temperature superconducting pancake test coil under transient heating *IEEE Trans. Appl. Supercond.* **11** 1852-5

[25] Haid B J, Lee H, Iwasa Y, Oh S S, Kwon Y K and Ryu K S 2002 Design analysis of a solid nitrogen cooled "permanent" high-temperature superconducting magnet system *Cryogenics* **42** 617-34

[26] Haid B J, Lee H, Iwasa Y, Oh S S, Kwon Y K and Ryu K S 2002 A "permanent" high-temperature superconducting magnet operated in thermal communication with a mass of solid nitrogen *Cryogenics* **42** 229-44

[27] Nakamura T, Muta I, Okude K, Fujio A and Hoshino T 2002 Solidification of nitrogen refrigerant and its effect on thermal stability of HTSC tape *Physica C* **372-376** 1434-7

[28] Nakamura T, Higashikawa K, Muta I, Fujio A, Okude K and Hoshino T 2003 Improvement of dissipative property in HTS coil impregnated with solid nitrogen *Physica C* **386** 415-8

[29] Nakamura T, Higashikawa K, Muta I and Hoshino T 2004 Performance of conduction-cooled HTS tape with the aid of solid nitrogen–liquid neon mixture *Physica C* **412–414, Part 2** 1221-4

[30] Hales P, Jones H, Milward S and Harrison S 2005 Investigation into the use of solid nitrogen to create a "Thermal Battery" for cooling a portable high-temperature superconducting magnet *Cryogenics* **45** 109-15

[31] Bascuñán J, Lee H, Bobrov E S, Hahn S, Iwasa Y, Tomsic M and Rindfleisch M 2006 A 0.6 T/650 mm RT bore solid nitrogen cooled MgB_2 demonstration coil for MRI - A status report *IEEE Trans. Appl. Supercond.* **16** 1427-30

[32] Iwasa Y 2006 HTS and NMR/MRI magnets: Unique features, opportunities, and challenges *Physica C* **445-448** 1088-94

[33] Song J B, Kim K L, Kim K J, Lee J H, Kim H M, Kim W S, Yim S W, Kim H R, Hyun O B and Lee H G 2008 The design, fabrication and testing of a cooling system using solid nitrogen for a resistive high-T_c superconducting fault current limiter *Supercond. Sci. Technol.* **21** 115023

[34] Yao W, Bascuñán J, Kim W S, Hahn S, Lee H and Iwasa Y 2008 A solid nitrogen cooled MgB_2 "demonstration" coil for MRI applications *IEEE Trans. Appl. Supercond.* **18** 912-5

[35] Bascuñán J, Hahn S, Ahn M and Iwasa Y 2010 Construction and test of a 500 MHz/200 mm RT bore solid cryogen cooled Nb_3Sn MRI magnet *AIP Confer. Proc.* **1218** 523-30

[36] Kim K L, Song J B, Choi J H, Kim S H, Koh D Y, Seong K C, Chang H M and Lee H G 2010 The design and testing of a cooling system using mixed solid cryogen for a portable superconducting magnetic energy storage system *Supercond. Sci. Technol.* **23** 125006

[37] Yao W, Bascuñán J, Hahn S and Iwasa Y 2010 MgB_2 coils for MRI applications *IEEE Trans. Appl. Supercond.* **20** 756-9

[38] Song J B, Kim K J, Kim K L, Lee J H, Kim H M, Lee G H, Chang H M, Park D K, Ko T K and Lee H G 2010 Thermal and electrical stabilities of solid nitrogen (SN_2) cooled YBCO coated conductors for HTS magnet applications *IEEE Trans. Appl. Supercond.* **20** 2172-5

[39] Song J-B and Lee H 2012 Mixed cryogen cooling systems for HTS power applications: A status report of progress in Korea University *Cryogenics* **52** 648-55

[40] Iwasa Y, Bascuñán J, Hahn S and Park D K 2012 Solid-cryogen cooling technique for superconducting magnets of NMR and MRI *Phys. Proc.* **36** 1348-53

[41] Song J B, Kim K L, Yang D G and Lee H G 2012 Thermal and electrical stabilities of YBCO coated conductor tapes in a solid argon-liquid nitrogen mixed cooling system *J. Supercond. Nov. Magn.* **25** 1431-40

[42] Kim K L, Song J B, Choi Y H, Yang D G, Yu I K, Park M W and Lee H G 2013 The effects of liquid cryogen on the thermal/electrical characteristics of a GdBCO coil in a mixed cryogen cooling system *IEEE Trans. Appl. Supercond.* **23** 4700405

[43] Patel D, Md Shahriar Al H, Khay Wai S, Qiu W, Kobayashi H, Zongqing M, Seong Jun K, Hong J, Jin Yong P, Choi S, Maeda M, Shahabuddin M, Rindfleisch M, Tomsic M, Dou S X and Kim J H 2016 Evaluation of persistent-mode operation in a superconducting MgB_2 coil in solid nitrogen *Supercond. Sci. Technol.* **29** 04LT2

[44] Patel D, Hossain M S A, Qiu W, Jie H, Yamauchi Y, Maeda M, Tomsic M, Choi S and Kim J H 2017 Solid cryogen: a cooling system for future MgB_2 MRI magnet *Scientific Reports* **7** 43444

[45] Iwasa Y 2009 *Case studies in superconducting magnets, design and operation issues* (New York: Springer)

[46] Dipak Patel, Md Shahriar Al Hossain, Wenbin Qiu, Hyunseock Jie, Yusuke Yamauchi, Minoru Maeda, Mike Tomsic, Seyong Choi and Kim J H 2017 Solid cryogen: a cooling system for future MgB_2 MRI magnet *Sci. Rep. (Accepted)*

[47] Ueno E, Kato T and Hayashi K 2014 Race-track coils for a 3 MW HTS ship motor *Physica C* **504** 111-4

[48] Järvelä J, Stenvall A, Mikkonen R and Rindfleisch M 2011 Contact resistance simulations and measurements of MgB_2 – MgB_2 lap joints *Cryogenics* **51** 400-7

[49] Patel D, Maeda M, Choi S, Kim S J, Shahabuddin M, Parakandy J M, Hossain M S A and Kim J H 2014 Multiwalled carbon nanotube-derived superior electrical, mechanical and thermal properties in MgB_2 wires *Scr. Mater.* **88** 13-6

[50] Thomas S, Varghese N, Rahul S, Devadas K M, Vinod K and Syamaprasad U 2012 Enhancement of bending strain tolerance and current carrying property of MgB_2 based multifilamentary wires *Cryogenics* **52** 767-70